Research Square

Preprints are preliminary reports that have not undergone peer review.
They should not be considered conclusive, used to inform clinical practice,
or referenced by the media as validated information.

Specifically Designed Amine Functional Group Doped Sludge Biochar for Inorganic and Organic Arsenic Removal

Chih-Kuei Chen
National I-Lan University
Nhat-Thien Nguyen (nguyennhatthien333@gmail.com)
National Taipei University of Technology https://orcid.org/0000-0001-5906-1957
Thuy-Trang Le
Duy Tan University
Cong-Chinh Duong
National Taipei University of Technology
Thi-Thanh Duong
Ho Chi Minh City University of Technology: Truong Dai hoc Bach khoa Dai hoc Quoc gia Thanh pho Ho Chi Minh

Research

Keywords: Hospital sludge, biochar, As(III), C2H7AsO2, DETA-SBC, density functional theory

Posted Date: December 4th, 2020

DOI: https://doi.org/10.21203/rs.3.rs-117105/v1

License: This work is licensed under a Creative Commons Attribution 4.0 International License.
Read Full License

Specifically designed amine functional group doped sludge biochar for inorganic and organic arsenic removal

Chih-Kuei Chen[1,2], Nhat-Thien Nguyen[3,*], Thuy-Trang Le[4], Cong-Chinh Duong [3,5] and Thi -Thanh Duong[6]

[1]*Department of Environmental Engineering, National I-Lan University, Ilan 26047, Taiwan*

[2]*Continental Water Engineering Corporation, Taipei 10608, Taiwan*

[3]*Institute of Environmental Engineering and Management, National Taipei University of Technology, Taipei 10608, Taiwan*

[4]*Faculty of Environment and Chemical Engineering, Duy Tan University, Da Nang 500000, Viet Nam*

[5]*Southern Institute of Water Resources Research, Ho Chi Minh 700000, Viet Nam*

[6]*Faculty of Environment and Natural Resources, Ho Chi Minh City University of Technology, Ho Chi Minh 700000, Viet Nam*

ABSTRACT

Usages of hospital sludge as a biochar adsorbent for wastewater treatment plants were investigated. Microwave carbonization was used to carbonize the sludge and then chemically activated with $ZnCl_2$ to increase surface area and porosity. A newly designed amine functional group's (DETA) doped sludge biochar carbon (SBC) presents effective inorganic arsenic (As(III), As_2O_3) and organic arsenic (p-ASA, $C_2H_7AsO_2$) adsorption in water. The pore volume, pore size distribution and specific surface area were determined by performing nitrogen adsorption-desorption measurements (BET). The Fourier transform infrared (FTIR) of the SBC was recorded to study the functional groups at room temperature. The composition of SBC was further determined by X-ray photoelectron spectroscopy (XPS). In order to understand the effect of amine functional complexes on arsenic adsorption, the adsorption mechanism of As_2O_3 and p-ASA on SBC surfaces modified with amine functional complexes was studied using density functional theory (DFT). Results showed that both physical and chemical adsorption of As_2O_3 and p-ASA on SBC surfaces occurred. The participation of amine functional complexes greatly promoted the surface activity of SBC surface and its adsorption capacity on arsenic. The physical adsorption energies of As_2O_3 and p-ASA on SBC surface with amine functional complexes were -38.4 and -32.8 KJ mol^{-1}, respectively. Other hand, the chemical adsorption energies of As_2O_3 and p-ASA on SBC surface with amine functional complexes were -92.9 KJ mol^{-1} and -98.5 KJ mol^{-1}, respectively.

Keywords: Hospital sludge, biochar, As(III), $C_2H_7AsO_2$, DETA-SBC, density functional theory.

**Corresponding author Email: nguyennhatthien333@gmail.com*

1. Introduction

Biochar has been identified as an effective adsorbent that can be used to remove various heavy metals dissolved in water, because the specific surface area and micro-porous structures of biochar are high. It hosts several surface functional groups, such as carboxyl (-COOH), hydroxyl (-OH) and amino (-NH_2), for adsorbing heavy metal effectively [1, 2]. These groups can work through electron donation, cation exchange, electrostatic attraction, or surface complexation to effectively remove heavy metals [3]. Recent studies have focused on the use of potential adsorbents, the utilization of sewage sludge [4], waste tire rubber [5], natural lignocellulose materials [6-8], doum stone [9], clays and their minerals [10], agriculture and industrial waste [12-13] as cheap and environment friendly materials has attracted increasing attention [14]. An alternative carbon source is readily available in the form of hospital sludge, which is currently managed as a waste in Taiwan. The amount of hospital sludge in the country has steadily increased, thus forcing the government to spend a significant amount of money on managing this waste. According to the previous study, it needs to spend a lot of time, more than 24 hours, to prepare biochar from hospital sludge with traditional methods, such as pyrolysis and calcination with N_2. It is important to shorten the time of preparing biochar within 15 min to get abundant products with feasible methods, such as microwave technology.

In other hand, natural weathering processes, volcanic eruptions, gold mining, biological activity, burning of fossil fuels, smelting of metal ores, desiccants, wood preservatives and agricultural pesticides, and many other anthropogenic activities are responsible for the presence of arsenic in water [15]. Arsenic is toxic and induces hyper-pigmentation, muscle weakness, skin thickening, neurological disorders and human cancer. Drinking contaminated groundwater is the principal route of human exposure. Therefore, the arsenic level for drinking water has been reduced by the WHO to 10 μg L^{-1} [16-19]. In addition, As(III) is more toxic than As(V) since the former binds to single but with higher affinity to nearby groups of

sulfhydryls that associate with a variety of proteins and inhibit their activity and given its electronic structure, As(III) is more stable than As(V) [15, 20].

Most ground state electronic structure calculations of molecules, atoms and solids are carried out using the density functional theory (DFT) method today. DFT is a valuable tool to study the mechanisms of interaction at the solid liquid interface. In the Zhang and Liu (2019) research, DFT-based quantum chemistry methods were used to explore the mechanism of adsorption of As(III) on the surface of ferric oxide. The results show that O-top and O-hollow sites on the α-ferric oxide acted as the active sites for As(III) adsorption, and the O-top activity is higher. The breakage of the As-O bond in the As(III) is the critical stage of As(III) adsorption, which is checked by comparing binding energy from various adsorption sites [21]. In the study of Fan et al. (2019), DFT calculations were investigated for the mechanisms of As(III) adsorption on the CaO surface under oxygen atmosphere. These reactions could be categorized as three forms according to the energy barrier with the goal to represent the strength of the necessary reaction temperature. Also the number of superficial CaO occupied by As(III) is considered to describe the adsorption reaction equation [22]. Gao et al. (2018) conducted a theoretical calculation on the effect on arsenic adsorption over carbonaceous surfaces of functional oxygen complexes and found that modified carbonaceous surfaces are highly adsorbent, which is highly consistent with experimental evidence [23]. According to the previous study, the mechanism of inorganic arsenic and organic arsenic adsorption on the carbon surface of biochar prepared from hospital sludge is hardly any theoretical study. Therefore, the adsorption mechanism of amine functional complexes for arsenic adsorption over biochar carbon sludge needs to be very clearly demonstrated. The inorganic arsenic and organic arsenic adsorption mechanisms on SBC and amine functional material were systematically investigated using DFT calculation. The objectives of this work are (a) to prepare sludge biochar carbon and amine functional material, such as SBC and DETA-SBC for developing key reaction between arsenic and

modified biochar; (b) to characterize sludge biochar carbon with BET, FTIR and XPS for verifying the mechanisms for adsorbing arsenic; (c) to obtain optimum operation conditions by assessing the effect of different DETA amount on adsorbing inorganic and organic arsenic; (d) to investigate the intra-particle diffusion parameters of arsenic adsorption for developing arsenic adsorption mechanisms; (e) to systematically calculate adsorption energy, bond distance and adsorbed structure through DFT.

2. Materials and methods

2.1. Starting materials and chemicals

Hospital sludge was obtained from Far Eastern Memorial Hospital water treatment plant at New Taipei city (1 ton day^{-1}) in Taiwan, respectively. The sludge was carbonized in a microwave carbonization reactor. The microwave generator was used by Zhuzhou Wavelane Technology Co., Ltd. (1000 W, Model Wemax A1). The sludge slurries were crushed and filtered (particle size of less than 0.1 mm) before activation. Hydrochloric acid (HCl), Zinc chloride ($ZnCl_2$), sodium hydroxide (NaOH) and diethylenetriamine (DETA) were purchased from Ke-Hua Chemical Reagent Co., Ltd. Inorganic arsenic and organic arsenic was obtained from As_2O_3 and $C_2H_7AsO_2$ (High-Purity Standards Co.). All chemical reagents were of analytical grade and directly used as received without further purification. Ultrapure water was obtained for the preparation of all solutions.

2.2. Preparation of DETA-SBC

DETA-SBC was prepared following the method as described above. In brief, most of the sludge moisture was removed in the decanter after pretreatment in a microwave oven at 1000 W for 30 min to obtain absolute preparation materials. To obtain the activated material, 50%$ZnCl_2$ and the as-synthesized carbonized sludge was added in 150 mL of deionized water, and stirred at 85±5 °C for 2 hr.

The mixture was dehydrated in an oven at 110±5 °C for 24 hr and then pyrolyzed in a horizontal tubular furnace under nitrogen flow at 500±5 °C for 2 hr. Then, 10 g of SBC was mixed with different amounts of DETA (including 0.7, 2.0, 3.3, 4.6 and 5.9%) solution, and stirring for 2 hr. The mixture again was dehydrated in an oven at 110±5 °C for 24 hr after filtered and rinsed by deionized water.

2.3. Materials characterization

The pore volume, pore size distribution and were specific surface area determined by performing nitrogen adsorption-desorption measurements with an ASAP 2020 apparatus by using Barrett-Joyner-Halenda (BJH) and Brunauer-Emmett-Teller (BET) calculation methods. The Fourier transform infrared (FTIR, NiCoLET- iS10) of the biochar carbon was recorded to study the functional groups at room temperature. The composition of biochar carbon was further determined by X-ray photoelectron spectroscopy (XPS).

2.4. Adsorption performance assessment

Adsorption isotherm experiments were carried out in 100 mL adsorption system. The porous adsorbents were mixed with 50 mL of the appropriate arsenic solution under 25 °C for 60 min. The solution was filtered with using a membrane filter (pore size 0.45 μm). In addition, an inductively coupled plasma atomic emission spectroscopy (ICP-AES) with a detection limit for arsenic of 10 ppb was used to evaluate the residual arsenic in the aqueous solutions. The test data were regularly calibrated using standard solution in order to obtain accurate data.

The exact amount of adsorbed As per adsorbent unit mass was determined by weight balance as follows:

$$q_e = [(C_o - C_e)/W] \times V \quad (1)$$

Where, the equilibrium adsorption capacity is q_e(mg g^{-1}), V (mL) is the volume of As solution, W (mg) is the amount of adsorbent used in the experiments, C_o (mg L^{-1}) is the initial concentration of As and the balance concentration measured after adsorption stands for C_e (mg L^{-1}).

2.5. DFT model and computation detail

The SBC surface is doped with DETA group to form other DETA-SBC structures. The two pollutants (As_2O_3 and $C_2H_7AsO_2$) are adsorbed on the above DETA-SBC structures respectively after 10ns molecular dynamics simulation. Finally adsorption systems were constructed in the same cubic simulation lattice built with their dimensions of x = 10 Å, y = 10 Å, and z = 14 Å.

In Materials Studio 2018, all the density functional theory (DFT) calculations in this analysis were carried out using the DMol3 software kit. The terms of exchange and correlation were determined in the form proposed by Perdew, Burke, and Ernzerhof (PBE) using the Generalized Gradient Approximation (GGA) [24]. The core DFT semi-core pseudo potential (DSPP) method was utilized to calculate the core treatment of DETA, for other elements, the all-electron method was applied [25]. Solvation effects were incorporated by COSMO solvation model for all the systems with water as solvent. The adsorption energy of pollute molecules on DETA-SBC surface (E_{ads}) was calculated by the following equation [26]:

$$E_{ads} = E_{DETA\text{-}SBC\text{-}pollute} - (E_{DETA\text{-}SBC} + E_{pollute}) \quad (2)$$

Where, $E_{DETA\text{-}SBC}$ and $E_{pollute}$ respectively represent the energies of the DETA-SBC surface and the single pollute molecule, and the $E_{DETA\text{-}SBC\text{-}pollute}$ is the total energy of pollute- DETA-SBC complex.

According to Formula (2), a negative value of E_{ads} indicates that the process is an exothermic reaction and high negative value corresponds to a stronger interaction, which indicates more heat release and a more stable product.

3. Results and discussion

3.1. Characterization of materials

The best activation ratio of carbonized sludge over $ZnCl_2$ was found to be 1:1, and the results are listed in Table I. The surface area, pore volume, and pore size of the un-activated SBC composites were estimated to be 96 m^2g^{-1}, 0.73 cm^3g^{-1} and 5.06 nm, respectively. In contrast, the surface area, pore volume, and pore size of the 50%$ZnCl_2$-SBC_2 composites were estimated to be 525 m^2g^{-1}, 0.35 cm^3g^{-1} and 8.71 nm, respectively. In the IPCC description, the isotherms belonged to Type IV and suggested that N_2 was condensed in the pores at high relative pressure [27]. The changes in the functional groups of SBC before and after activation was analyzed by FTIR spectroscopy, it is seen that chemicals are well mixed with raw material as show in Figure 1. The -OH and N-H stretching vibration band are characteristic peaks of the amine group at about 3410 cm^{-1} [28] and C-O vibrations at 1760 cm^{-1} are disappeared for all SBC [29]. The appearance of peaks at 2930 and 2849 cm^{-1} in the spectrum were attributed to C-H stretching vibration in -CH and -CH_2 [28]. The band at 1620 cm^{-1} can be ascribed to C-C aromatic ring stretching vibration [29]. The band at 1473- 1435 cm^{-1} is ascribed to C-H bending vibrations in CH_2 groups [28]. The existence of bands about 1040-1100 cm^{-1} which was assigned to SiO_2 represented the nature of the feedstock, and these bands were observed in all biochar carbon [30]. There is a weak vibration band between 765-530 cm^{-1}, which is judged as an aromatic structure. Due to the large amount of organic

matter in the sludge, the chemical structure is composed of a large number of different atoms. Therefore, there are more functional groups. The XPS spectrum of the SBC hybrid sample is shown in Figure 2 (a), which shows the characteristic peak of C, N and O. The results show that double-bonding carbons for SBC are assigned the highest peak at 285 eV and result from non-functionalized carbon. The peak of approximately 285 eV binding energy for SBC is a result of single carbon bonding [31, 32]. In the DETA-SBC high-resolution N1s region, as shown in Figure 2(b), due to neutral amine nitrogen (−NH−) from the DETA chains, there is an extreme peak at 399 eV. When the DETA is doped on SBC, the main component of the N1s peak shifts to 400 eV, refers to the amine nitrogen (-NH-) [33].

3.2. Effect of DETA content

In this section, it discusses the impact of the amino group density grafted on the SBC loading number. The density of amino groups will vary with the different DETA material added during the synthesis procedure. Different DETA content, including 0.7, 2.0, 3.3, 4.6 and 5.9% was evaluated with 3.0 g L^{-1} of DETA-SBC at 0.5 mg L^{-1} As(III) and p-ASA, pH 3 and 30 min contact time. Figure 3 shows the removal efficiency of As(III) and p-ASA significantly increases from 41% to 86% and 52% to 97%, respectively, with increasing DETA content from 0.7 to 5.9%. However, the removal efficiency is not changed obviously with increasing the DETA content from 4.6 to 5.9%. In this study, it shows that the amino groups impregnated on SBC significantly can enhance the adsorption capacity for As (III) and p-ASA. The higher DETA content does not increase the removal efficiency, but can increase the cost of the material preparation. The adsorption capacity of As (III) and p-ASA was calculated as 1.64 and 2.04 mg g^{-1}, respectively, with 4.6%DETA-SBC.

3.3. Intra-particle diffusion model

The rate limiting step was calculated with the intra-particle diffusion model to better understand the adsorption mechanism. The results fitted and the parameters derived from this model as shown in Figure 4. Their correlation coefficient (R^2) obtained fell within the range of 0.618-0.986. The plots were multi-linear and show their various processes of adsorption. The first line shows that a sharper portion is due to the spread of arsenic through the solution to the external adsorbent surface, as show in the intra-particle diffusion model. The second line defines the gradual stage of adsorption, in which intra-particle diffusion limits the rate. This result is similar with the results of Xiong et al. (2017) [7].

3.4. The physi-adsorption configurations of As(III) and p-ASA on SBC

Finite benzene clusters from single layer activated carbon structure were used in this analysis to simulate surface models of SBC, as shown in Figure 5 (a). First, the adsorption of inorganic and organic arsenic to SBC is predicted to be unstable, as SBC is inefficient for the removal of arsenic. As observed in Figure 5 (b-c) and Table II, the As_2O_3 and $C_2H_7AsO_2$ are adsorbed onto SBC with E_{ads} value of -21.1 and -27.5 KJ mol^{-1}, respectively, in different conformations, indicating a physical adsorption between arsenic and SBC surface since E_{ads} value is smaller than -50 KJ mol^{-1} [23]. The bond distance of C-O bond is 3.61 Å in configuration Figure 5 (b) and the bond distance of C-O bond is 3.41 Å in configuration Figure 5 (c). It illustrate that $C_2H_7AsO_2$ adsorbed onto SBC is stronger than As_2O_3 adsorbed onto SBC verified by its larger E_{ads} value.

3.5. The physi-adsorption configurations of As(III) and p-ASA on DETA-SBC

The results for the adsorption of As_2O_3 and $C_2H_7AsO_2$ on the DETA doped onto SBC surface are summarized in Table II and Figure 6. The DETA doped onto SBC surface with E_{ads} values of up to -291.7 KJ mol^{-1}, the adsorption energies of DETA-SBC are all large enough to anchor DETA atom firmly. The

bond distance of C-N bond is 1.61 Å, in configuration Figure 6 (a). Interestingly, when the DETA doped onto SBC is used for adsorption of both anionic As_2O_3 and $C_2H_7AsO_2$ a high improvement in the adsorption power is achieved. Results show the As_2O_3 and $C_2H_7AsO_2$ are adsorbed onto DETA -SBC surface with E_{ads} values of up to -38.4 and -32.8 KJ mol^{-1}, respectively, in different conformations, indicating a physical adsorption between arsenic and DETA-SBC surface. The bond distance of N-As bond is 2.26 Å in configuration Figure 6 (b) and the bond distance of N-As bond is 3.92 Å in configuration Figure 6 (c). It illustrate that $C_2H_7AsO_2$ adsorbed onto DETA-SBC is also stronger than As_2O_3 adsorbed onto DETA-SBC verified by its larger E_{ads} value.

3.6. The possible chemi-adsorption configurations of As(III) and p-ASA on DETA-SBC

The results for the adsorption of inorganic and organic arsenic on the DETA-SBC surface displays all the obtained conformations in Figure 7 and Table III shows the bond type, bond distances and adsorption energies. Six possible adsorption configurations were considered in Figure 7 (a–f) to obtain the As_2O_3's most stable adsorption configuration. The mostly mono-dentate conformations have been found. The bond distances of N-As and N-O are in the range between 2.05–1.82 Å and 2.32–1.96 Å, respectively, which are shorter for the trivalent compounds in compliance with the increased adsorption energies, between -52.4 and -92.9 KJ mol^{-1}. The conformation in Figure 7 (c) is higher adsorption energy than that of the others. Additionally, six ground state adsorption conformations for $C_2H_7AsO_2$ were obtained, as show in Figure 8 (a–f). With regards to the adsorption of $C_2H_7AsO_2$ on the surface of DETA-SBC, $C_2H_7AsO_2$ gained electron, while DETA and biochar carbon lost electron. Accordingly, the adsorption of $C_2H_7AsO_2$ on the surface of DETA-SBC all belong to stable chemisorptions. Configuration Figure 8 (d) tends to have a weak chemical reaction within, which corresponds with -53.4 KJ mol^{-1} of adsorption

energy. Otherwise, adsorption energy of configuration Figure 8 (c) is -98.5 KJ mol^{-1}, this suggests a strong chemical adsorption between the surface $C_2H_7AsO_2$ and DETA-SBC.

In this study, the reaction mechanism is divided into three pathways. The first pathway is the attachment of arsenic ions onto the SBC via physical adsorption, which may be attributed to Van der Waals forces [34]. The second pathway is the arsenic species adsorption, which is primarily based on the SBC surface chemistry and the aqueous phase chemistry. Furthermore, The SBC has acidic and basic groups, so that the surface load density can be positive at low pH [35]. The third pathway is the attachment of amine functional groups onto the surface of SBC and their replacement with oxygen groups, which is a modification method for producing strong adsorbents toward heavy metals [36]. The surface charging of amino-functional SBC is positive because of the protonation effect of amine groups when the pH solution is lower than pKa (pKa^{+}_{NH4}= 10). Afterwards, the electrostatic attraction between arsenic anions and protonated amino groups contributes to the adsorption efficiency [6].

3.7. Mechanism discussion of arsenic adsorption by DETA-SBC material

The mechanism for the adsorption of arsenic by biochar has been proposed with the results obtained from the experimental data, as presented in Figure 9. The reaction mechanism is divided into three pathways. The first pathway is the attachment of arsenic ions into the pore of DETA-SBC material via physical adsorption. Second pathway, the surface load of amino-functional biochar is positive because of the protonation effect of amine groups when the pH solution is lower than pKa. Then, the electrostatic attraction between arsenic anions and protonated amino groups contributes to the adsorption [6], as shown in the formula (3) and (4). The third pathway is the attachment of amine functional groups onto the surface of adsorbents and their replacement with oxygen groups, which is a modification method for producing

strong adsorbents toward heavy metals [36]. This reaction mechanism is also consistent with XPS analysis results.

$$M\text{-}NH_3 + H_2AsO_4 = M\text{-}NH_2 \cdot H_3AsO_4 \quad (3)$$

$$M\text{-}NH_3 + H_3AsO_3 = M\text{-}NH_3 \cdot H_3AsO_3 \quad (4)$$

The surface composition of the pristine and amino functionalized DETA-SBC materials was analyzed by XPS. The core level spectrum of N 1s of the DETA-SBC sample reveals the binding energy peaks at 398.5 eV, 399.6 eV and 400.4 eV corresponding to C-NH_3^+, C-NH_2 and C-N=C core levels, respectively. The percentages of C-NH_3^+, C-NH_2 and C-N=C relative to the total N were calculated, as shown in Figure 10. Similar types of satellite peaks were observed earlier by Ederer et al. (2017) [37]. By comparing Figure 10 (a-b), it can be seen that the relative content of C-NH_3^+ after the reaction was reduced from 46.69% to 28.68%; meanwhile, that of C-NH_2^+ increased from 22.48% to 59.75%, which implied that during the adsorption experiment, the C-NH_3^+ that were coupled with the SBC were likely to react with the As anions contaminants adsorbed on the surface of the electrode particles, causing a decrease in the C-NH_3^+ content.

4. Conclusion

These findings clearly show the feasibility of processing biochar from hospital sludge as a carbon source. The biochar has homogeneous pores and high surface area (>520 m^2 g^{-1}). The removal efficiency of As(III) and p-ASA significantly increases with increasing DETA content from 0.7 to 4.6%. But, the removal efficiency is not changed obviously with increasing the DETA content from 4.6 to 5.9%. The amino groups impregnated on SBC significantly can enhance the adsorption capacity for As (III) and p-ASA. The DFT results showed that both physical and chemical adsorption of As_2O_3 and p-ASA on SBC

surface took place. The presence of amine functional complexes greatly promoted SBC surface activity and its adsorption potential on arsenic. The reaction mechanism is divided into three pathways.

Declarations

Availability of data and materials

All data generated or analyzed during this study are examined by our group and certified for several times.

Competing interests

The authors declare they have no competing interests.

Funding

Not applicable

Authors' contributions

Chih-Kuei Chen provided real test data, Thuy-Trang Le supported the test data, Cong-Chinh Duong wrote the paper, Thi -Thanh Duong analyzed the test data, and Nhat-Thien Nguyen organized the researched full structure. All authors read and approved the final manuscript.

Acknowledgements

The authors acknowledge financial supports form the Taiwan's Ministry of Science and Technology (MOST 107-2622-E-197-001 -CC3). First author acknowledges the Department of Environmental Engineering, National I–Lan University, Taiwan to support his research at the university.

Authors' information (optional)

1. Chih-Kuei Chen: Department of Environmental Engineering, National I-Lan University, I-Lan, 26047, Taiwan.

Continental Water Engineering Corporation, Taipei 10608, Taiwan.

2. Nhat-Thien Nguyen: Institute of Environmental Engineering and Management, National Taipei University of Technology, Taipei 10608, Taiwan.
3. Thuy-Trang Le: Faculty of Environment and Chemical Engineering, Duy Tan University, Da-Nang 500000, Viet Nam.
4. Cong-Chinh Duong: Institute of Environmental Engineering and Management, National Taipei University of Technology, Taipei 10608, Taiwan.

Southern Institute of Water Resources Research, Ho Chi Minh 700000, Viet Nam.

5. Thi-Thanh Duong: Faculty of Environment and Natural Resources, Ho Chi Minh City University of Technology, Ho Chi Minh 700000, Viet Nam.

References

1. Giri AK, Patel R, Mandal S. Removal of Cr(VI) from aqueous solution by Eichhornia crassipes root biomass - derived activated carbon. Chem Eng J. 2012;185:71–81.
2. Tan XF, Liu SB, Liu YG, Gu YL, Zeng GM, Hu XJ, Wang X, Liu SH, Jiang LH. Review biochar as potential sustainable precursors for activated carbon production: multiple applications in environmental protection and energy storage. Bioresour Technol. 2017;227:359–372.
3. Zhi M, Liu S, Hong Z, Wu N. Electrospun activated carbon nano-fibers for super capacitor electrodes. RSC Adv. 2014;82:43619–43623.
4. Acıkyıldız M, Gurses A, Karaca S. Preparation and characterization of activated carbon from plant wastes with chemical activation. Microporous Mesoporous Mater. 198;2014:45–49.
5. Karmacharya MS, Gupta VK, Tyagi I, Agarwal S, Jha VK. Removal of As(III) and As(V) using rubber tire derived activated carbon modified with alumina composite. J Mol Liq. 2016;216:836–844.
6. Hao L, Zheng T, Jiang J, Zhang G, Wang P. Removal of As(III) and As(V) from water using iron doped amino functionalized sawdust: Characterization, adsorptive performance and UF membrane separation. Chem Eng J. 2016;292:163–173.
7. Xiong Y, Tong Q, Shan W, Xing Z, Wang Y, Wen S, Lou Z. Arsenic transformation and adsorption by iron hydroxide/manganese dioxide doped straw activated carbon. Appl Surf Sci. 2017;416:618–627.
8. Owlad M, Aroua MK, Daud WMAW. Hexavalent chromium adsorption on impregnated palm shell activated carbon with polyethyleneimine. Bioresour Technol. 2010;101:5098–5103.

9. Hamed MM, Ali MMS, Holiel M. Preparation of activated carbon from doum stone and its application on adsorption of ^{60}Co and $^{152+154}Eu$: Equilibrium, kinetic and thermodynamic studies. J Environ Radioact. 2016;164:113-124.
10. Uddin MK. A review on the adsorption of heavy metals by clay minerals, with special focus on the past decade. Chem Eng J. 2017;308:438-462.
11. Kurniawan TA, Sillanpaa ME, Sillanpaa M. Nano adsorbents for remediation of aquatic environment: Local and practical solutions for global water pollution problems. Crit Rev Environ Sci Technol. 2012;42:1233–1295.
12. Ray PZ and Shipley HJ. Inorganic nano-adsorbents for the removal of heavy metals and arsenic: A review. RSC Adv. 2015;5:29885–29907.
13. Delgado CN and Mendez JR. Anchorage of iron hydro (oxide) nano particles onto activated carbon to remove As (V) from water. Water Res. 2012;46:2973-2982.
14. Mandal S, Sahu MK, Patel RK. Adsorption studies of arsenic(III) removal from water by zirconium polyacrylamide hybrid material (ZrPACM-43). Water Resour Ind. 2013;4:51–67.
15. Choong TSY, Chuah TG, Robiah Y, Koay FLG, Azni I. Arsenic toxicity, health hazards and removal techniques from water: An overview. Desalination. 2017;217:139–66.
16. Mohan D and Pittman CU. Arsenic removal from water/ wastewater using adsorbents – a critical review. J Hazard Mater. 2007;142:1–53.
17. Smith AH, Lingas EO, Rahman M. Contamination of drinking-water by arsenic in Bangladesh: a public health emergency. Bull World Health Organ. 2000;78:1093–103.
18. Ryu SR, Jeon EK, Yang JS, Baek K. Adsorption of As(III) and As(V) in groundwater by Fe–Mn binary oxide-impregnated granular activated carbon. J Taiwan Inst Chem Eng. 2017;72:62–69.
19. Aposhian HV, Maiorino RM, Dart RC, Perry DF. Urinary excretion of meso-2, 3-dimercaptosuccinic acid in human subjects. Clin Pharmaco Ther. 1989;45:520–526.
20. Zhang Y and Liu J. Density functional theory study of arsenic adsorption on the Fe_2O_3 (001) surface. Energy Fuels. 2019;33:1414−1421.
21. Fan Y, Weng Q, Zhuo Y, Dong S, Hu P, Li D. Theoretical study of As_2O_3 adsorption mechanisms on CaO surface. Materials. 2019;12:677-690.
22. Gao Z, Li M, Sun Y, Yang W. Effects of oxygen functional complexes on arsenic adsorption over carbonaceous surface. J Hazard Mater. 2018;360:436–444.
23. Perdew JP, Burke K, Ernzerhof M. Generalized gradient approximation made simple. Phys Rev Lett. 1997;77:3865-3868.
24. Delley B. Hardness conserving semilocal pseudopotentials. Phys Rev B. 2002;66:155125-15532.
25. Hu L, Peng Y, Wu F, Peng S, Li J, Liu Z. Tubular activated carbons made from cotton stalk for dynamic adsorption of airborne toluene. J Taiwan Inst Chem Eng. 2017;80:399–405.
26. Wang SJ. Pore size control of MCM-41. Master. National Central University. Institute of Chemistry. 2005.
27. Ma Y, Liu WJ, Zhang N, Li YS, Hong J, Sheng GP. Polyethylenimine modified biochar adsorbent for hexavalent chromium removal from the aqueous solution. Bioresour Technol. 2014;169:403–408.

28. Kilic M, Apaydin-Varol E, Putun AE. Adsorptive removal of phenol from aqueous solutions on activated carbon prepared from tobacco residues: Equilibrium, kinetics and thermodynamics. J Hazard Mater. 2011;189:397–403.
29. Jindo K, Mizumoto H, Sawada Y, Sanchez-Monedero MA, Sonoki T. Physical and chemical characterization of biochars derived from different agricultural residues. Biogeosciences, 2014;11:6613–6621.
30. Ma J, Zhu Z, Chen B, Yang M, Zhou H, Li C, Yu F, Chen J. One-pot, large-scale synthesis of magnetic activated carbon nanotubes and their applications for arsenic removal. J Mater Chem A. 2013;1:4662–4666.
31. Chen CC, Chen CF, Chen CM, Chuang FT. Modification of multi-walled carbon nanotubes by microwave digestion method as electro catalyst supports for direct methanol fuel cell applications. Electro Comm. 2007;9:159–163.
32. Yang BY, Cao Y, Qi FF, Li XQ, Xu Q. Atrazine adsorption removal with nylon6/ polypyrrole core-shell nanofibers mat: possible mechanism and characteristics. Nanoscale Res Lett. 2015;10:207- 220.
33. Nwosu FO, Olu-Owolabi BI, Adebowale KO. Kinetics and thermodynamic adsorption of Pb(II) and Cd(II) ions from used oil onto thevetia neriifolia nutshell active carbon. Current Res Chem. 2012;4:26-40.
34. Dobrowolski R and Otto M. Preparation and evaluation of Ni-loaded activated carbon for enrichment of arsenic for analytical and environmental purposes. Microporous and Mesoporous Mater. 2013;179:1–9.
35. Deliyanni EA, Kyzas GZ, Triantafyllidis KS, Matis KA. Activated carbons for the removal of heavy metal ions: A systematic review of recent literature focused on lead and arsenic ions. Open Chem. 2015;13:699–708.
36. Ederer J, Jano P, Ecorchard P, Tolasz J, Stengl V, Benes H, Perchacz M, Pop-Georgievski O. Determination of amino groups on functionalized graphene oxide for polyurethane nanomaterials: XPS quantitation vs. functional speciation. RSC Adv. 2017;7:12464- 12473.

Table I. The surface area and pore volume of materials.

Material	S_{BET} (m^2 g^{-1})	V_{meso} (cm^3 g^{-1})	d_p (nm)
SBC	96	0.73	5.06
33%$ZnCl_2$-SBC	378	0.27	7.25
50%$ZnCl_2$-SBC	525	0.35	8.71
60%$ZnCl_2$-SBC	516	0.34	7.66
67%$ZnCl_2$-SBC	436	0.29	6.87

Table II. E_{ads} value of As_2O_3 and $C_2H_7AsO_2$ adsorbed onto each material.

Material	Bond	Bond distance (Å)	E_{ads} (KJ mol^{-1})
SBC	C-As (b)	3.61	-21.1
	C-As (c)	3.41	-27.5
DETA-SBC	C- N (a)	1.61	-291.7
	N-As (b)	3.26	-32.4
	N-As (c)	2.92	-38.8

Table III. Adsorption energies of As_2O_3 and $C_2H_7AsO_2$ adsorbed onto DETA-SBC surface.

ɔllutant	ond	Bond distances (Å)	E_{ads} (KJ mol^{-1})
	-As (a)	2.05	-79.5
	-As (b)	2.13	-52.4
	- As (c)	1.82	-92.9
s_2O_3	-O (d)	2.32	-61.5
	-O (e)	2.13	-83.6
	-O (f)	1.96	-90.7
	-As (a)	2.16	-74.6
	-As (b)	2.12	-76.2
	-As (c)	1.91	-94.3
$_2H_7AsO_2$	-O (d)	2.23	-53.4
	-O (e)	2.14	-75.5
	-O (f)	1.92	-98.5

Figure captions

Figure 1. FTIR spectrums of (a) SBC, (b) 33%$ZnCl_2$-SBC, (c) 50%$ZnCl_2$-SBC, (d) 60%$ZnCl_2$-SBC and (e) 67%$ZnCl_2$-SBC.

Figure 2. XPS spectra of (a) SBC and (b) DETA-SBC.

Figure 3. Effect of grafted amino density on the adsorption performance.

Figure 4. Plot of the intra-particle diffusion equation for the adsorption of arsenic.

Figure 5. Configurations of As_2O_3 and $C_2H_7AsO_2$ adsorption on SBC surface.

Figure 6. Configurations of (a) As_2O_3 and (b) $C_2H_7AsO_2$ adsorption on DETA-SBC surface.

Figure 7. The possible adsorption configurations of As_2O_3 on DETA-SBC.

Figure 8. The possible adsorption configurations of $C_2H_7AsO_2$ on DETA-SBC.

Figure 9. The schematic diagram of mechanism for arsenate adsorption on DETA-SBC.

Figure 10. XPS of the N 1s state of amino functional present in DETA-SBC: (a) before and (b) after the As adsorption.

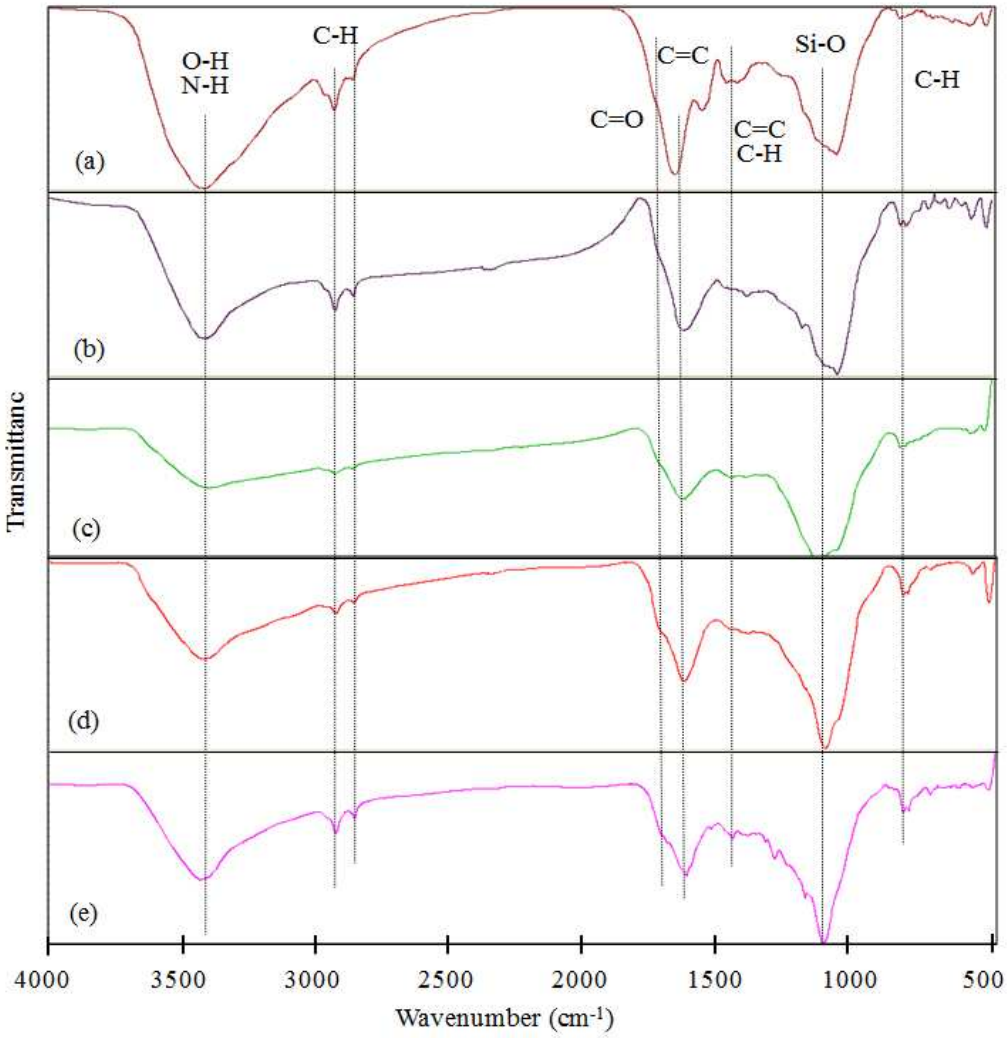

Figure 1. Chen et al.

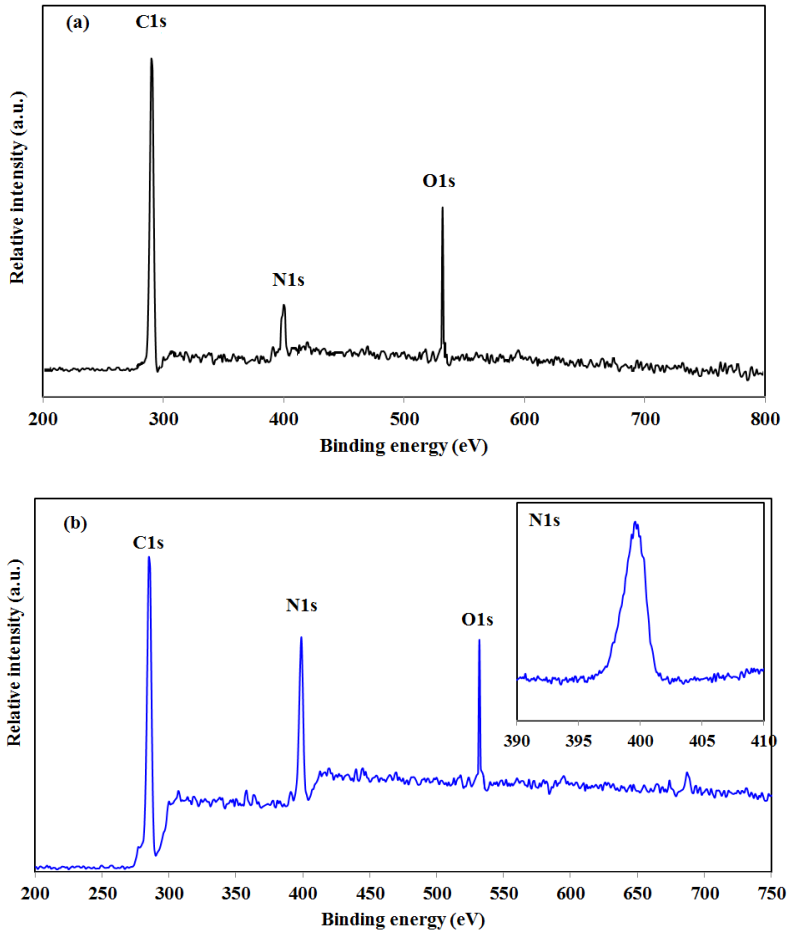

Figure 2. Chen et al.

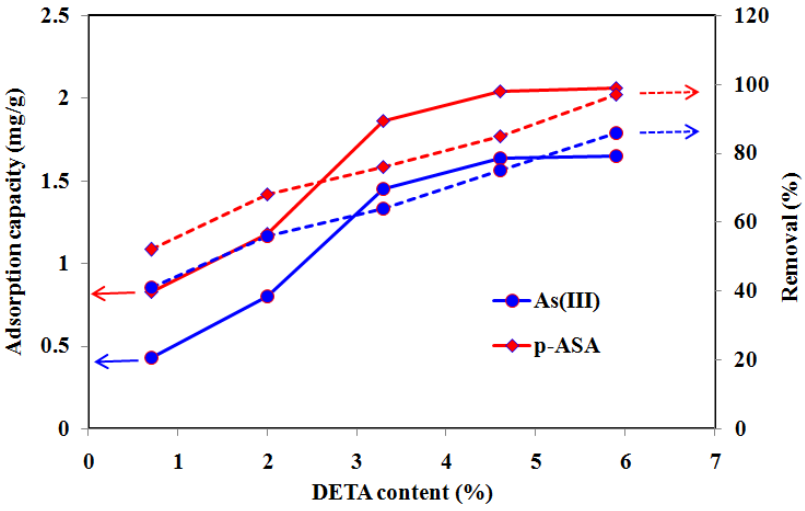

Figure 3. Chen et al.

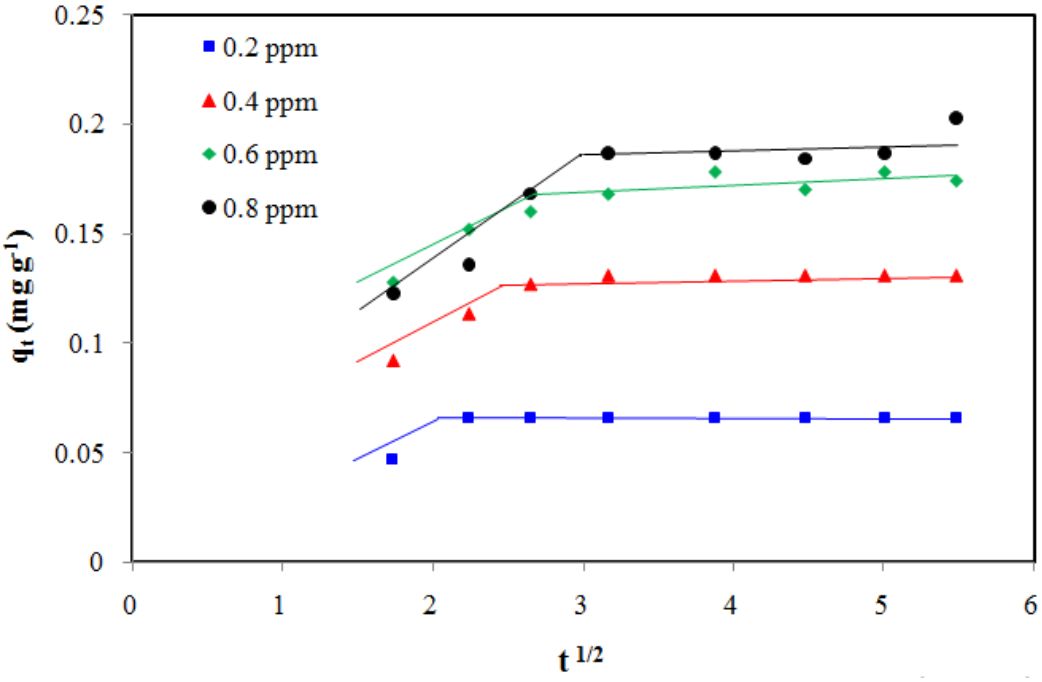

Figure 4. Chen et al.

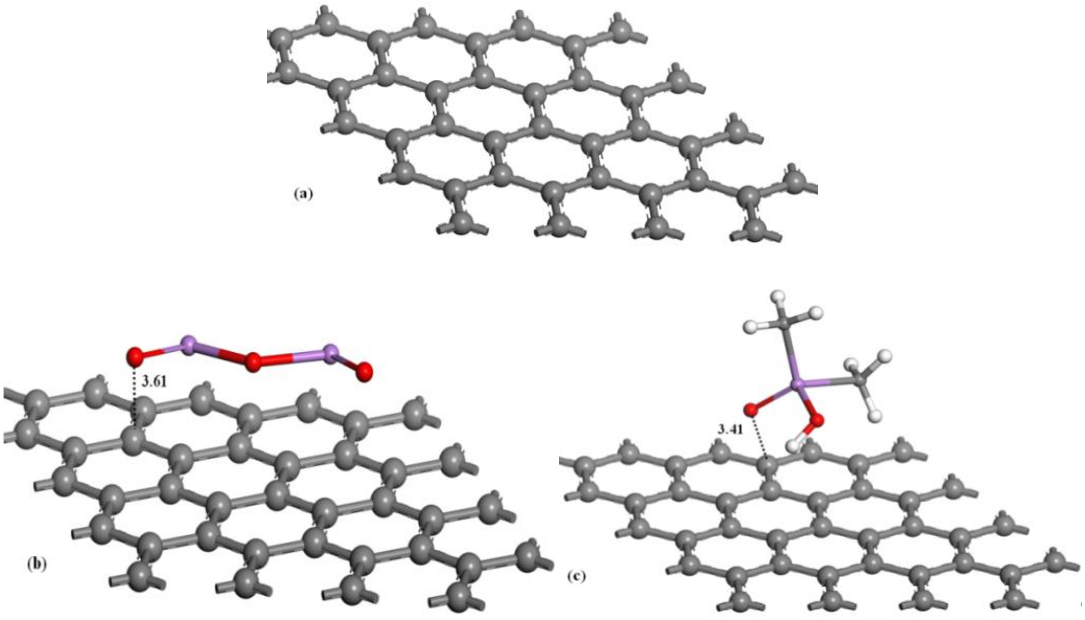

Figure 5. Chen et al.

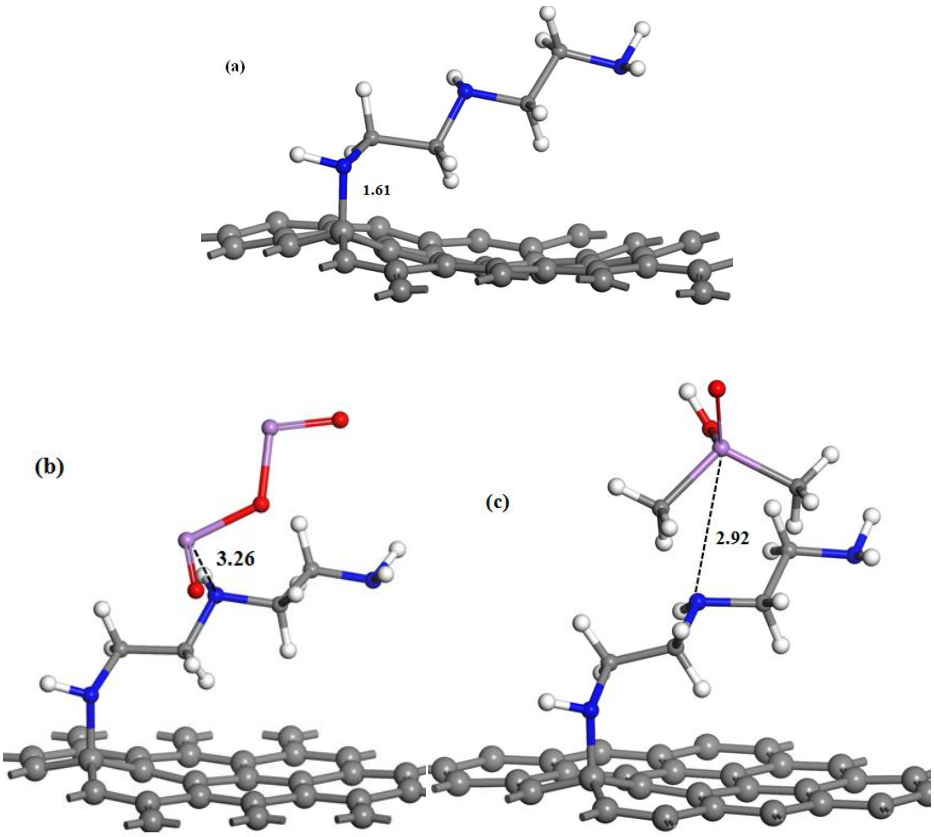

Figure 6. Chen et al.

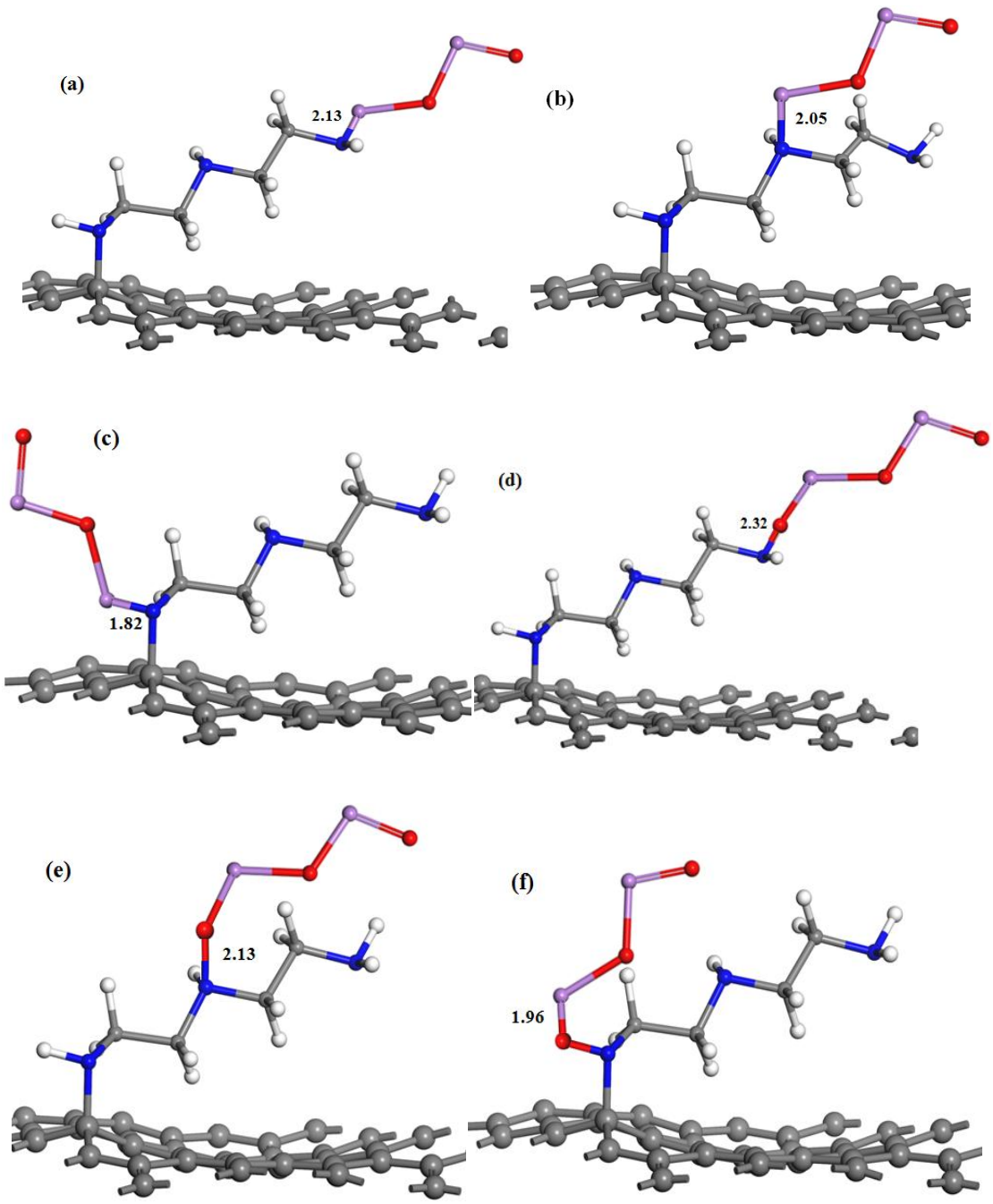

Figure 7. Chen et al.

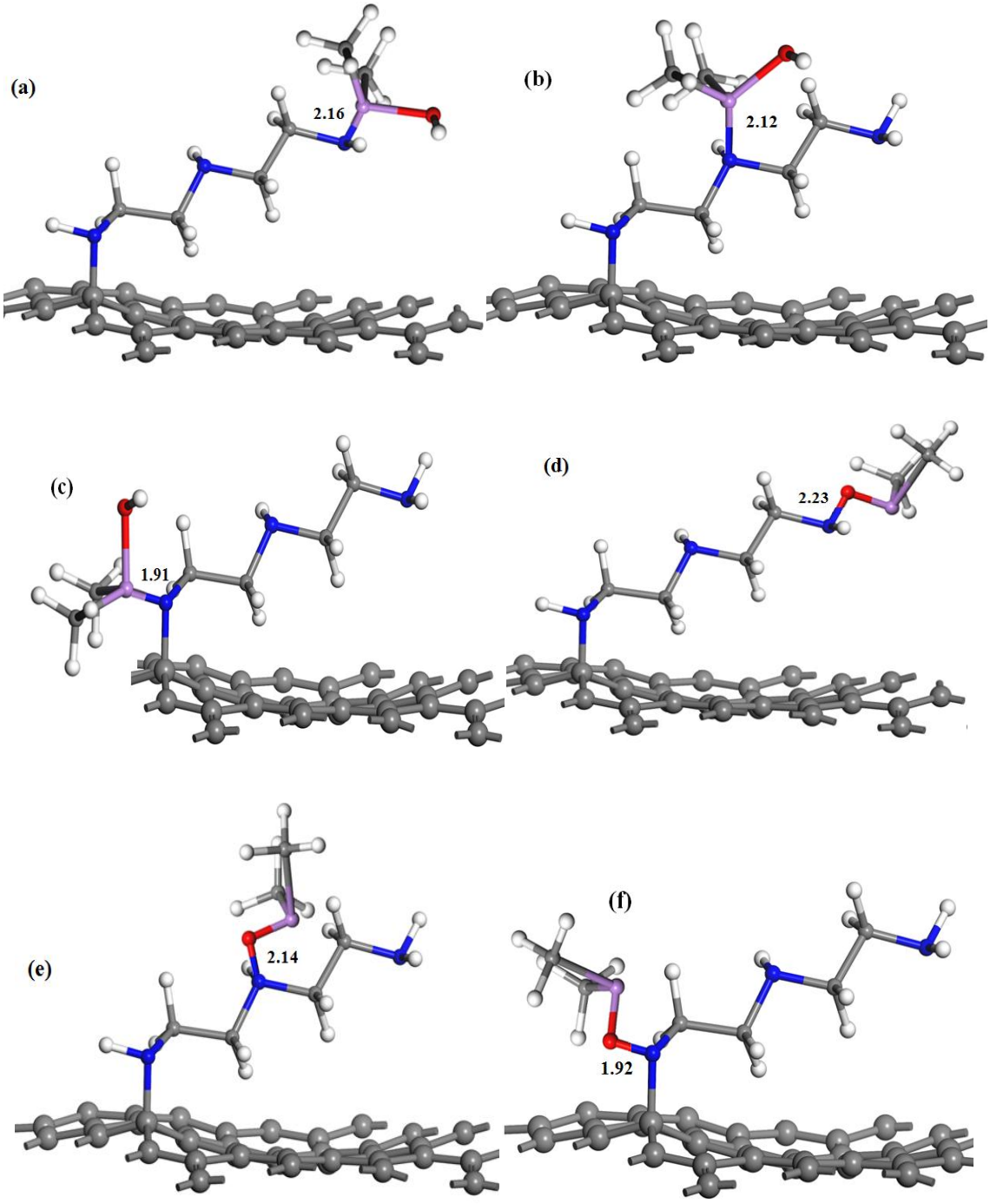

Figure 8. Chen et al.

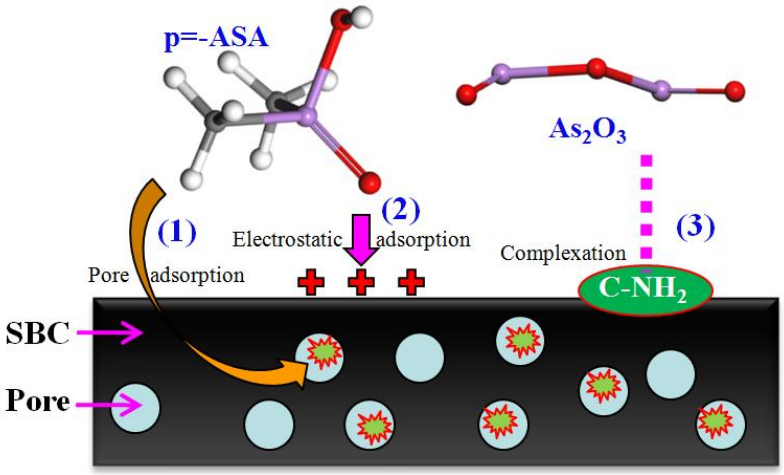

Figure 9. Chen et al.

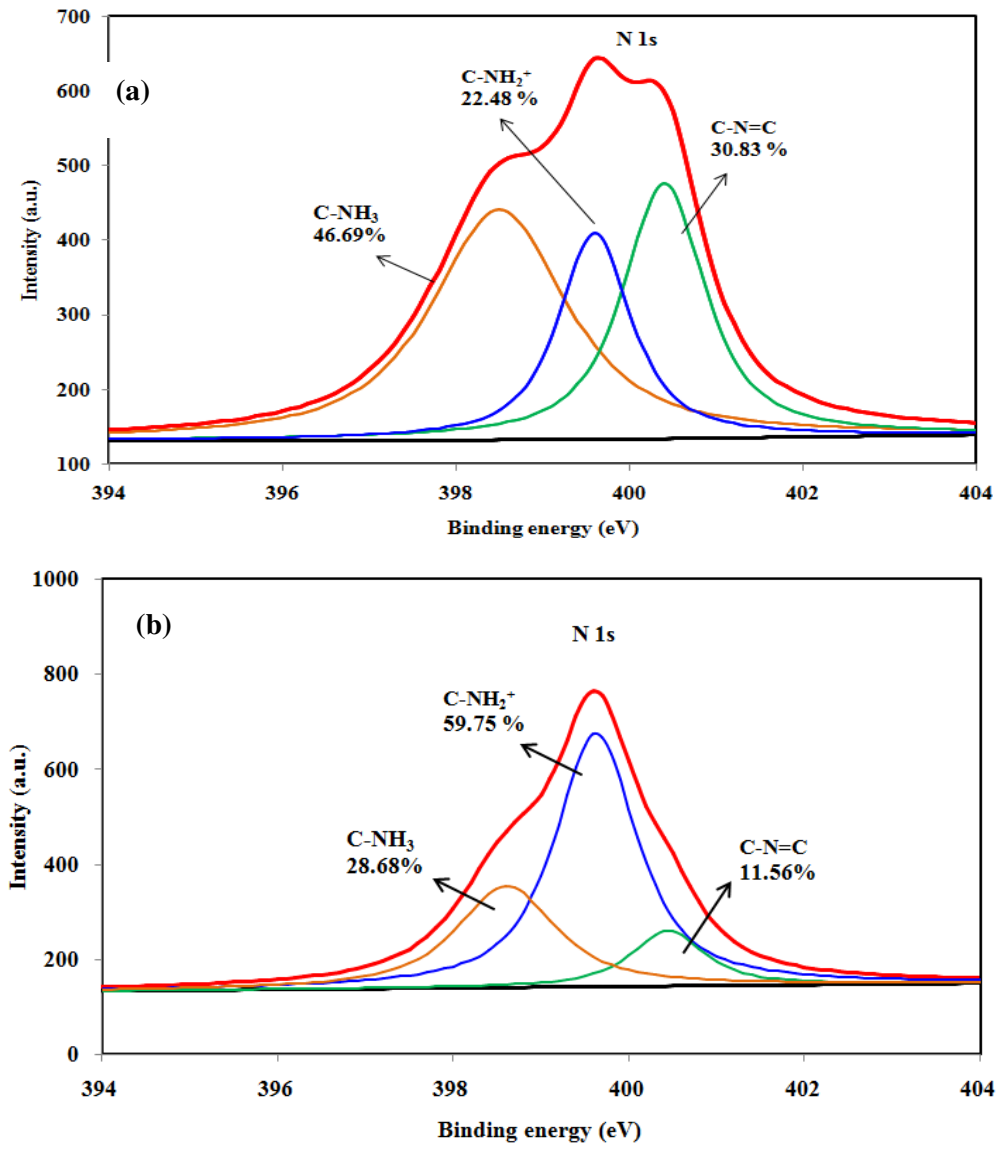

Figure 10. Chen et al.

Figures

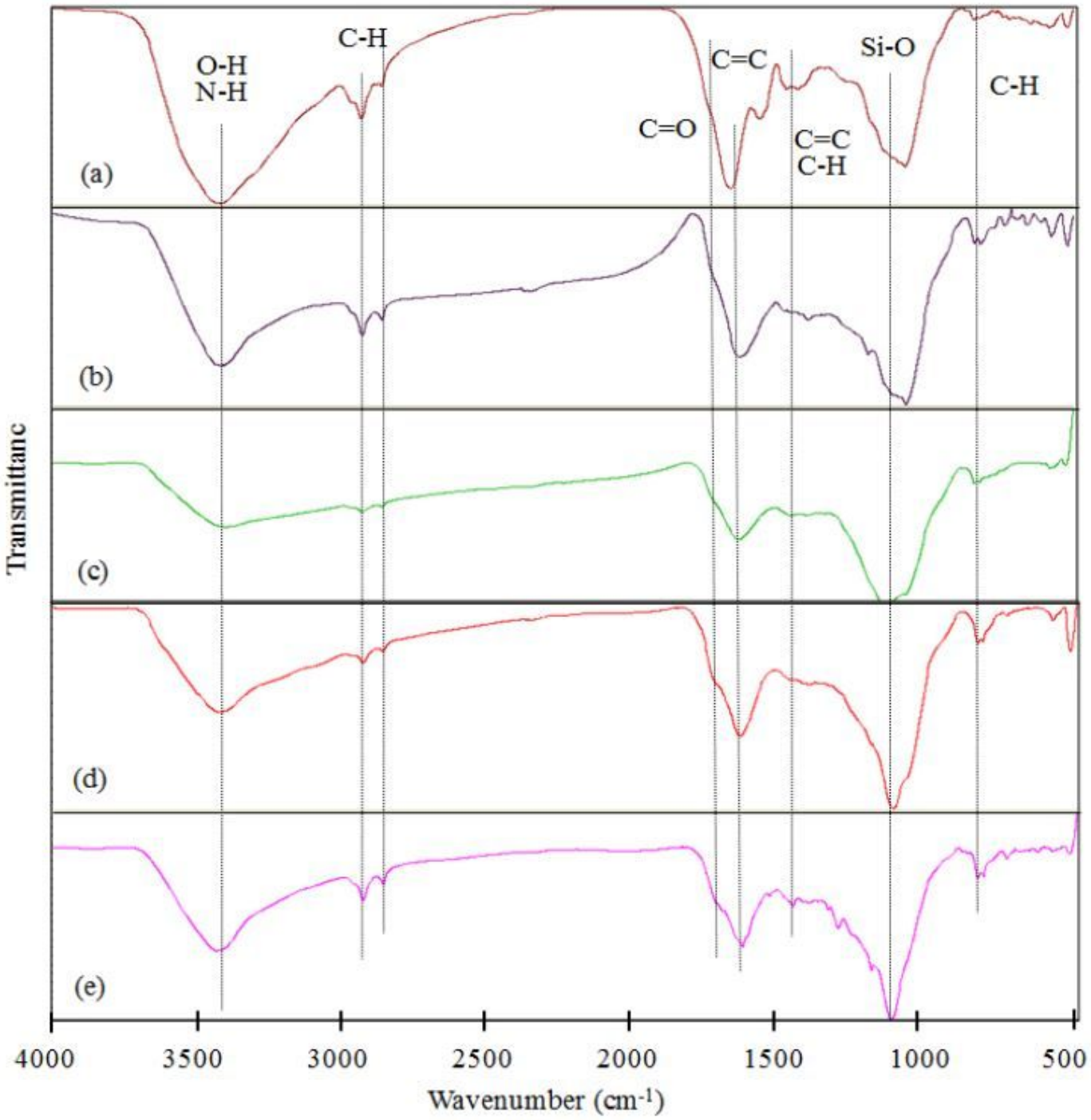

Figure 1

FTIR spectrums of (a) SBC, (b) 33%ZnCl2-SBC, (c) 50%ZnCl2-SBC, (d) 60%ZnCl2-SBC and (e) 67%ZnCl2-SBC.

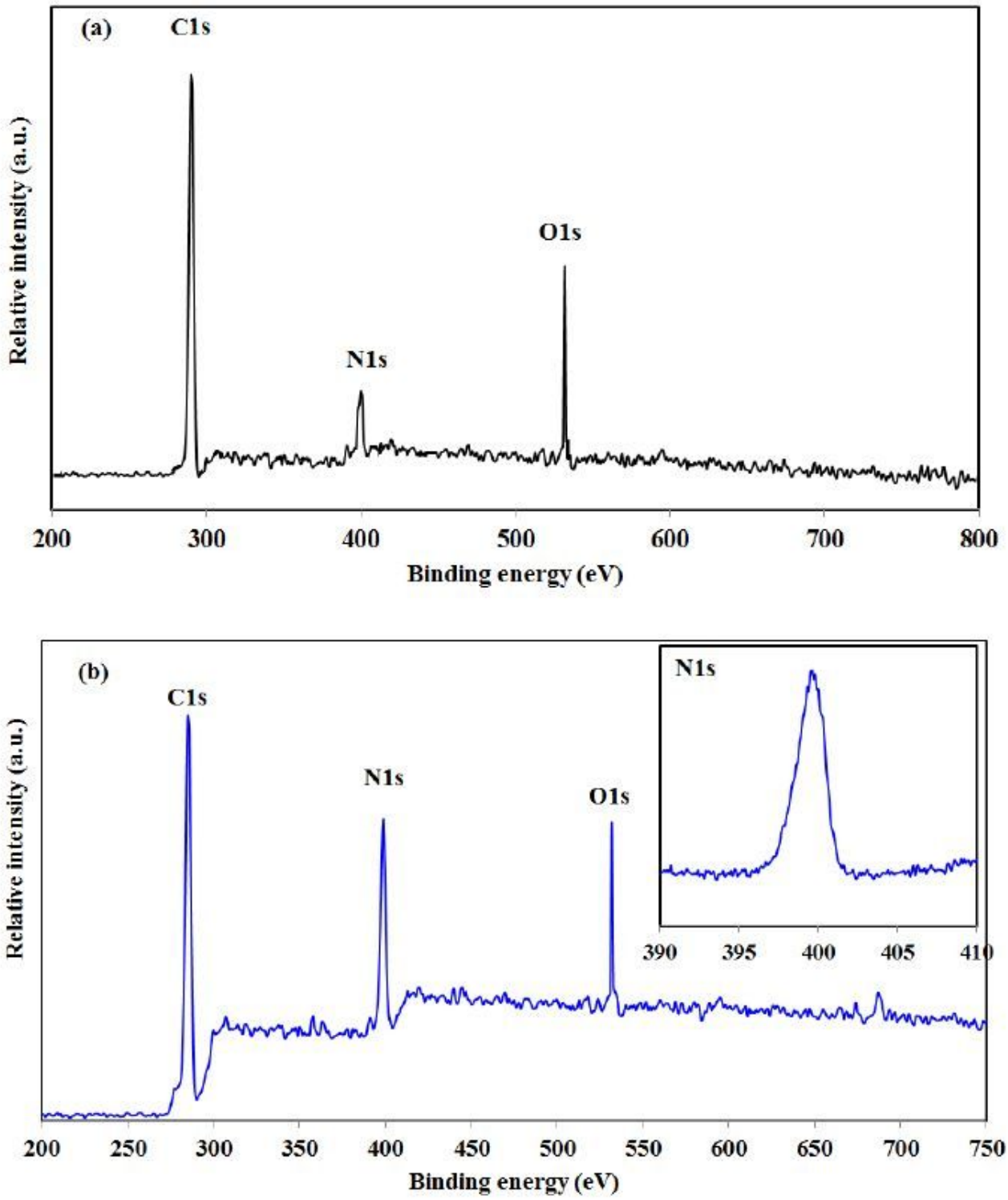

Figure 2

XPS spectra of (a) SBC and (b) DETA-SBC.

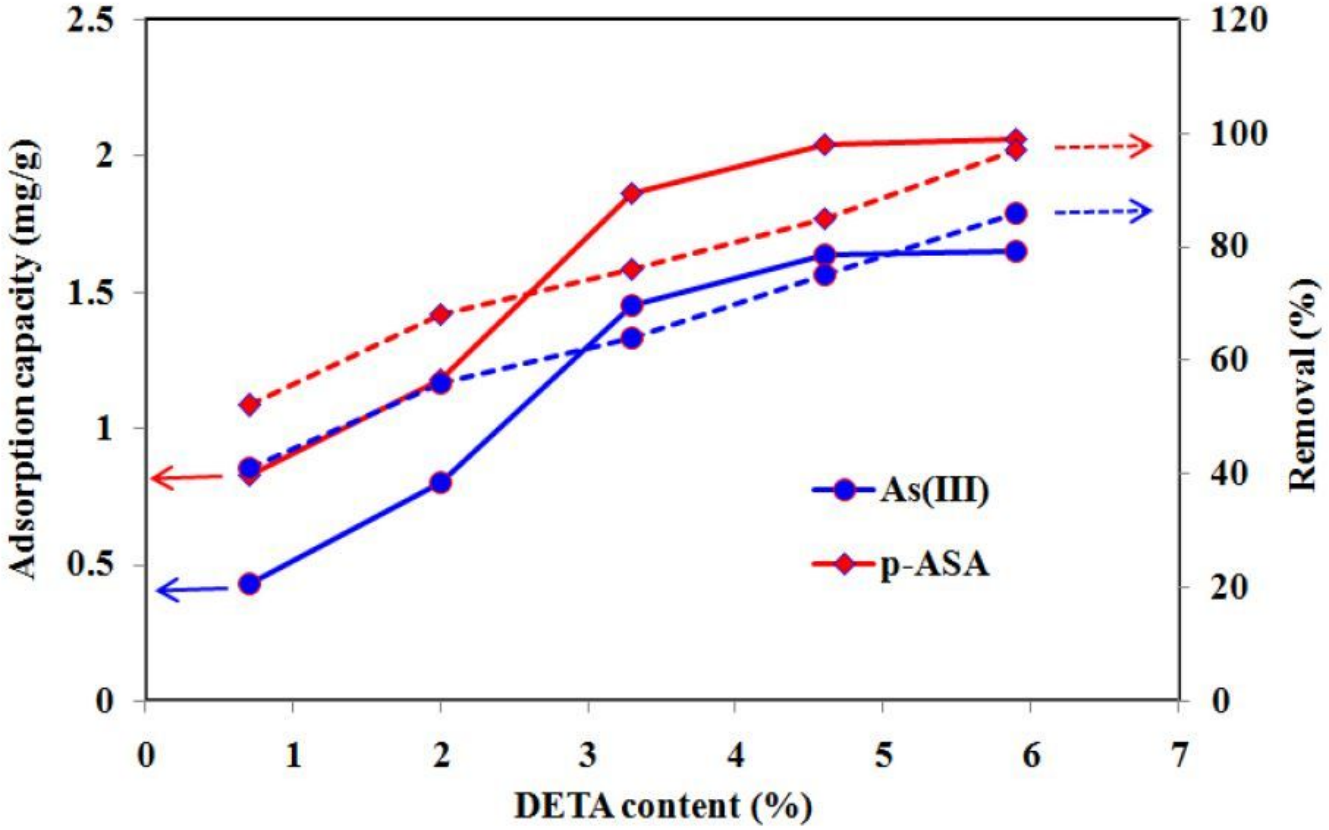

Figure 3

Effect of grafted amino density on the adsorption performance.

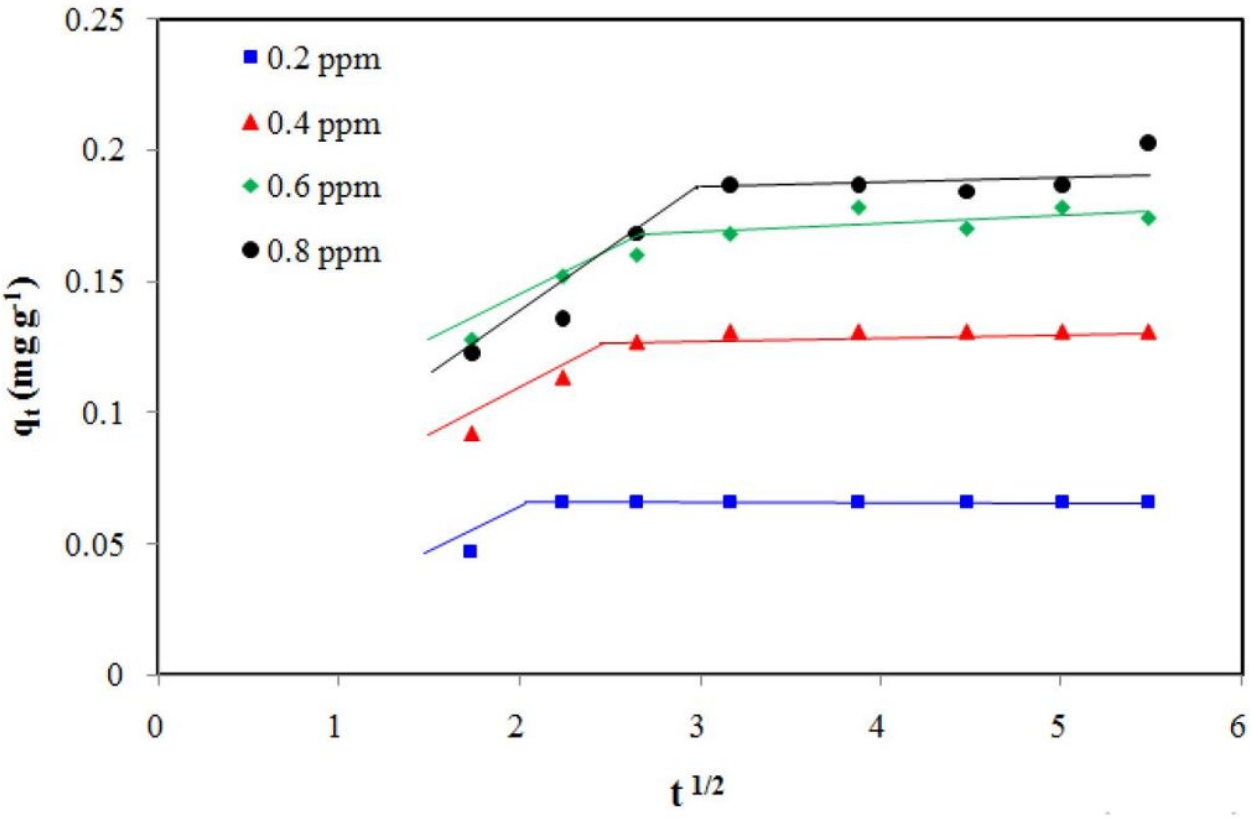

Figure 4

Plot of the intra-particle diffusion equation for the adsorption of arsenic.

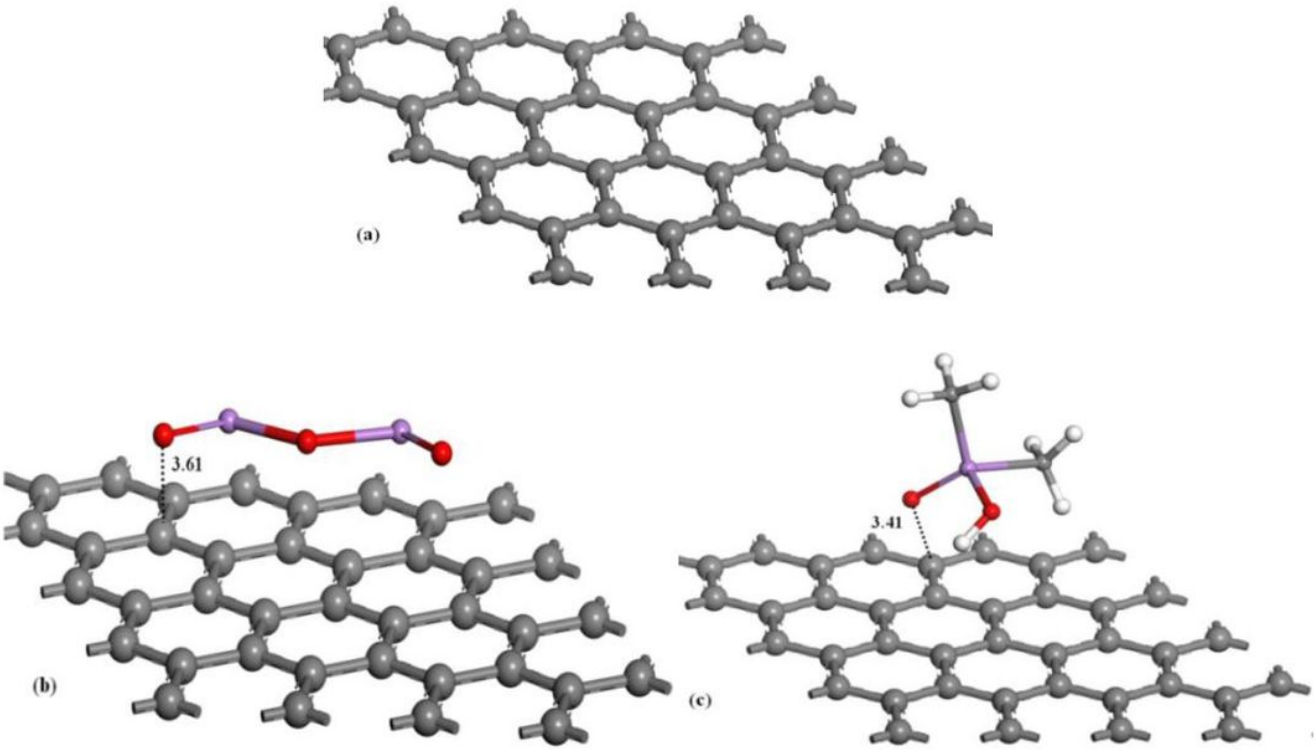

Figure 5

Configurations of As2O3 and C2H7AsO2 adsorption on SBC surface.

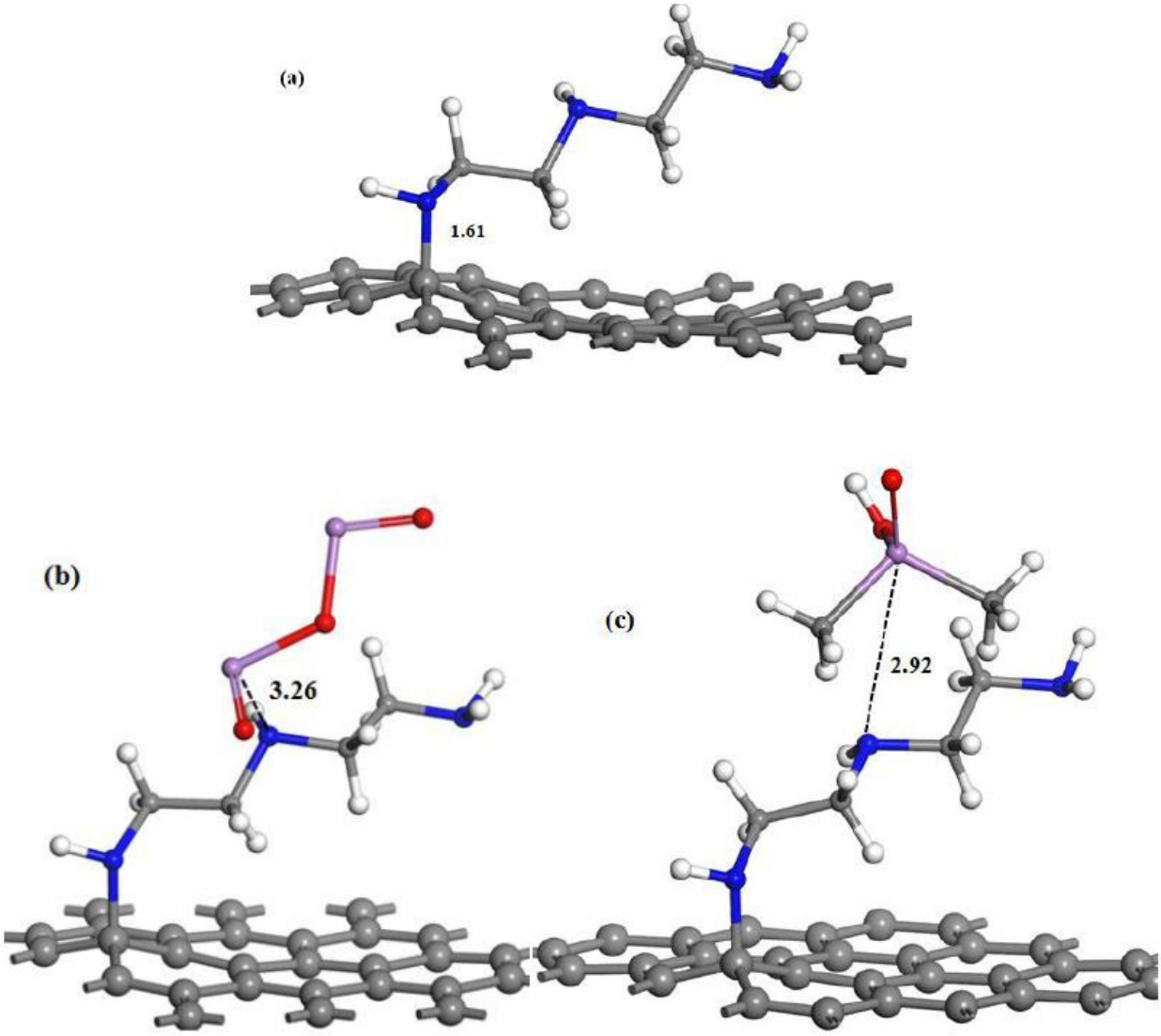

Figure 6

Configurations of (a) As2O3 and (b) C2H7AsO2 adsorption on DETA-SBC surface.

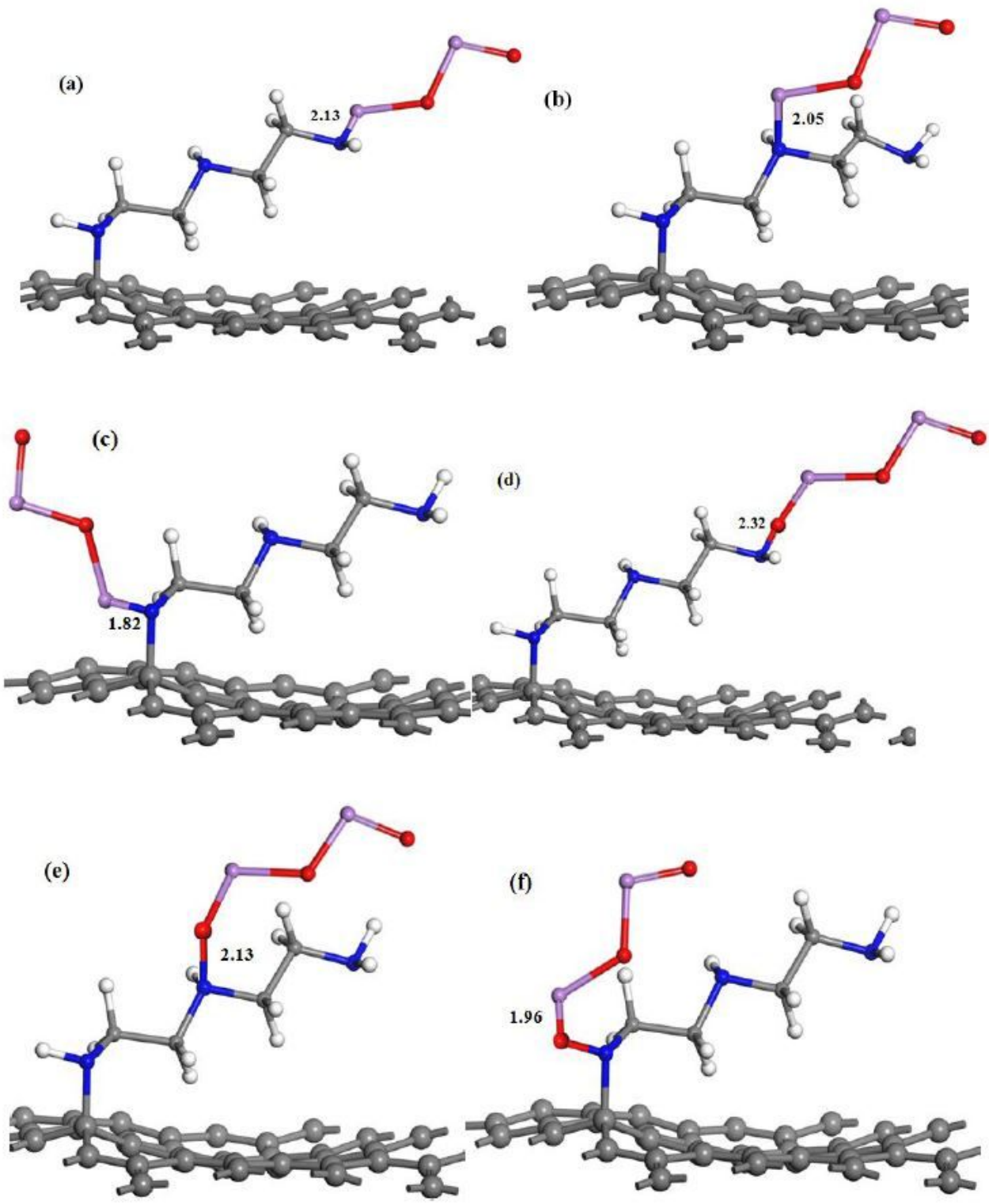

Figure 7

The possible adsorption configurations of As2O3 on DETA-SBC.

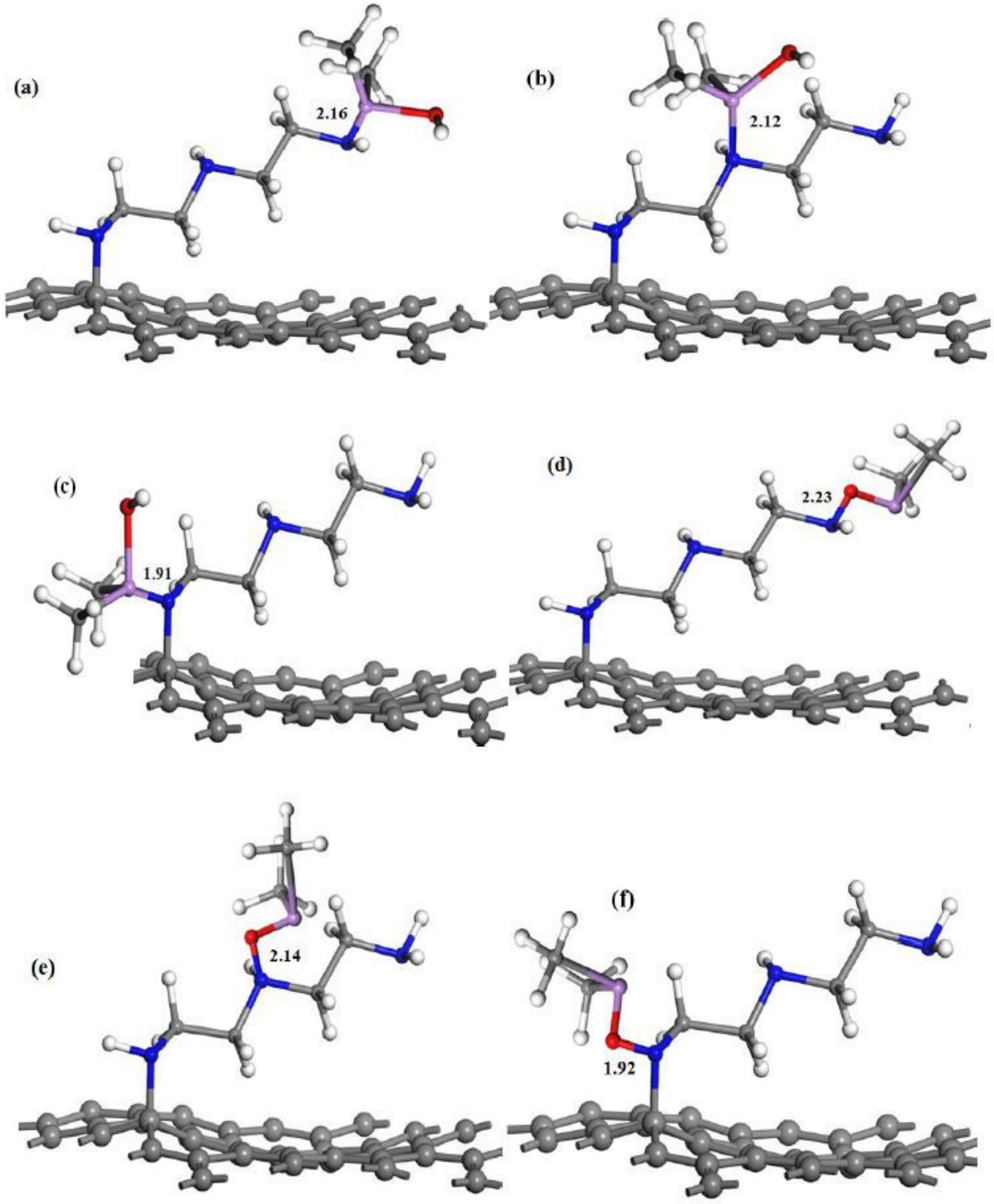

Figure 8

The possible adsorption configurations of C2H7AsO2 on DETA-SBC.

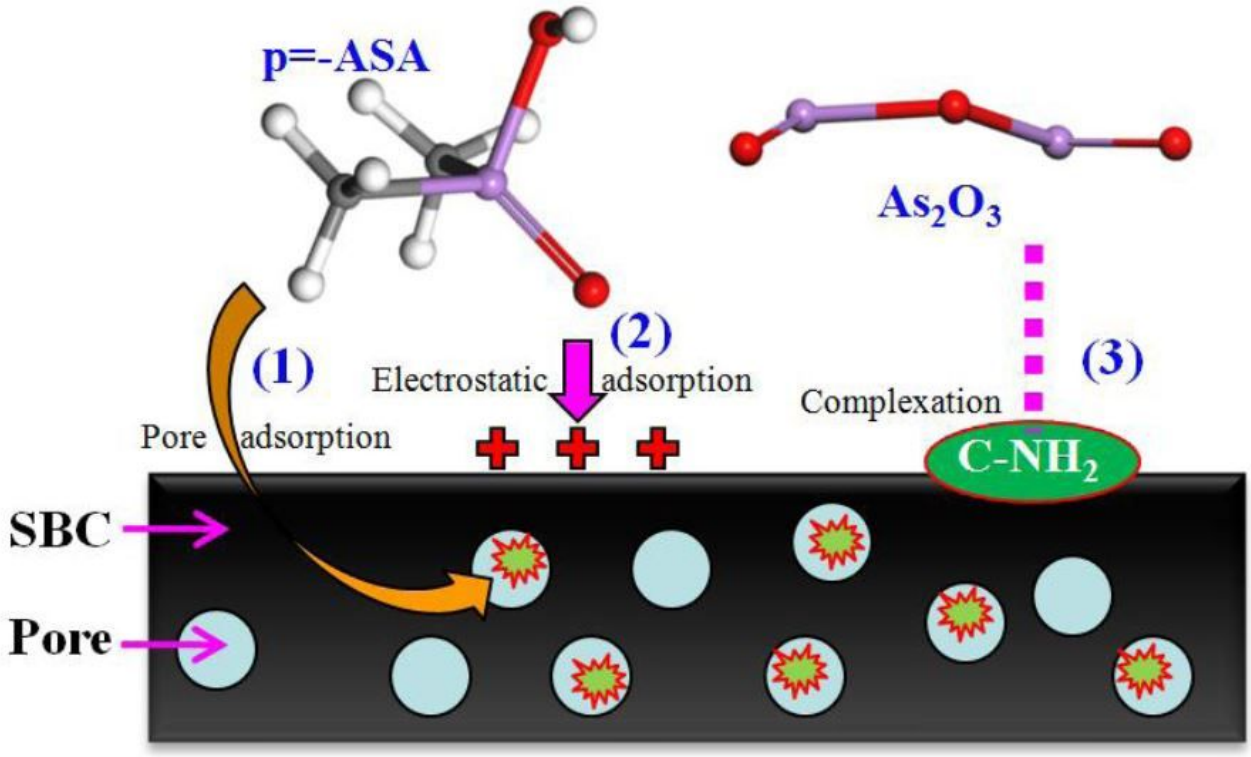

Figure 9

The schematic diagram of mechanism for arsenate adsorption on DETA-SBC.

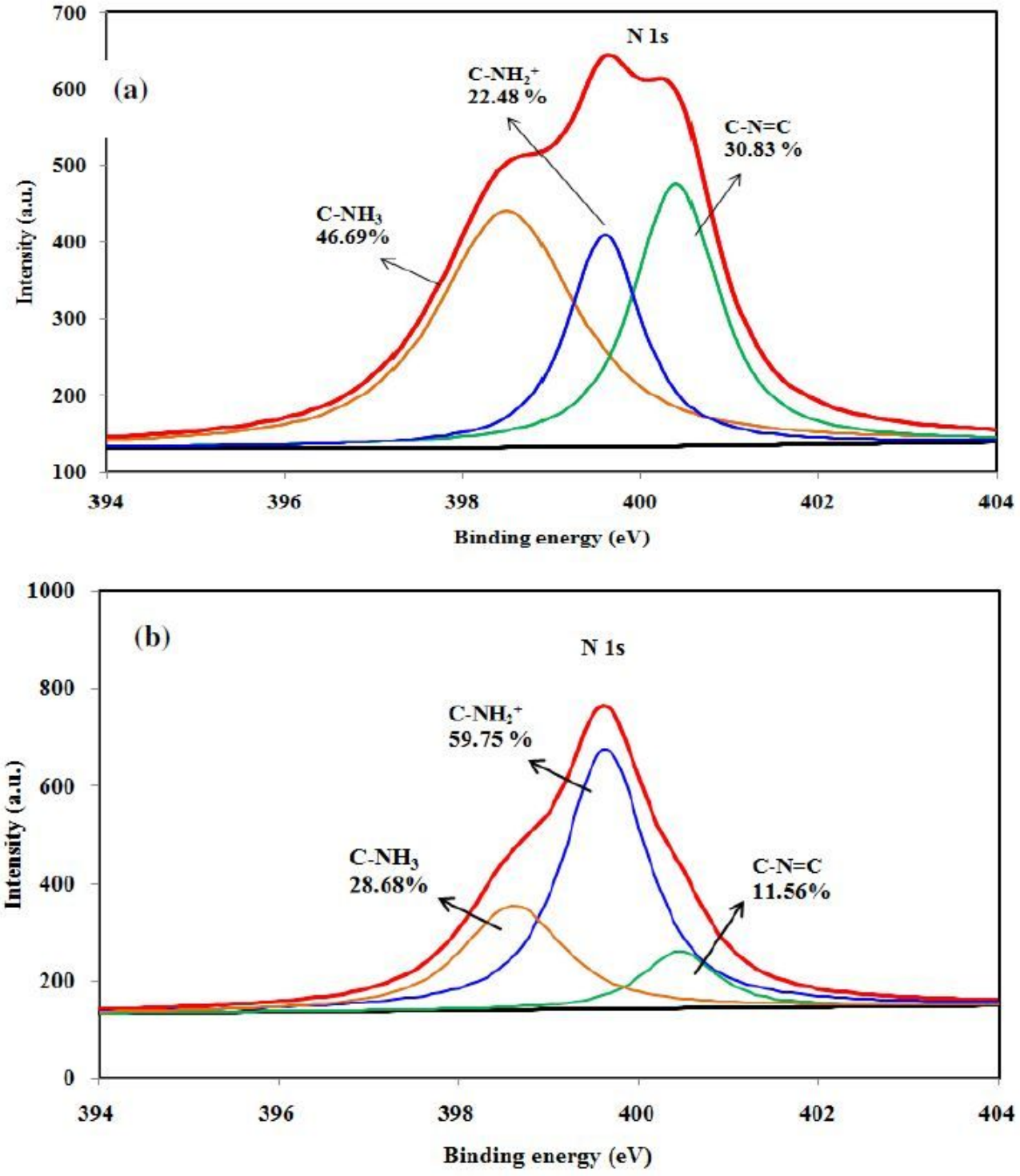

Figure 10

XPS of the N 1s state of amino functional present in DETA-SBC: (a) before and (b) after the As adsorption.